COSMIC-RAY TRANSPORT AND ANISOTROPIES

PETER L. BIERMANN[1,2,3,4,5], JULIA BECKER TJUS[6], EUN-SUK SEO[7], AND MATTHIAS MANDELARTZ[6]

[1] MPI for Radioastronomy, Auf dem Hügel 69, D-53121 Bonn, Germany
[2] Department of Physics & Astronomy, University of Alabama, Tuscaloosa, AL 35487, USA
[3] Institute of Experimental Nuclear Physics, Campus North, Karlsruher Institut für Technologie (KIT), D-76021 Karlsruhe, Germany
[4] Department of Physics, University of Alabama at Huntsville, AL 35899, USA
[5] Department of Physics & Astronomy, University of Bonn, D-53115 Bonn, Germany
[6] Ruhr-Universität Bochum, Fakultät für Physik & Astronomie, Theoretische Physik I, D-44780 Bochum, Germany
[7] Department of Physics, University of Maryland, College Park, MD 20742, USA

ABSTRACT

We show that the large-scale cosmic-ray anisotropy at $\sim$10 TeV can be explained by a modified Compton–Getting effect in the magnetized flow field of old supernova remnants. Cosmic rays arrive isotropically to the flow field and are then carried along with the flow to produce a large-scale anisotropy in the arrival direction. This approach suggests an optimum energy scale for detecting the anisotropy. Two key assumptions are that propagation is based on turbulence following a Kolmogorov law and that cosmic-ray interactions are dominated by transport via cosmic-ray-excited magnetic irregularities through the stellar wind of an exploding star and its shock shell. A prediction is that the amplitude is smaller at lower energies due to incomplete sampling of the velocity field and also smaller at larger energies due to smearing.

Key words: astroparticle physics – cosmic rays – ISM: structure – ISM: supernova remnants

1. INTRODUCTION

In the past few years, a number of cosmic-ray (CR) experiments have convincingly shown that the arrival directions of Galactic CR particles are not fully isotropic in the sky: a large-scale anisotropy with a dipole and quadrupole component was first observed in the northern hemisphere at an energy of several TeV (Amenomori et al. 2006; Guillian et al. 2007; Abdo et al. 2008, 2009). The same structure was later found in the southern hemisphere at a mean energy of 20 TeV (Abbasi et al. 2010). The large-scale anisotropy I, observed at several to tens of TeV energies, is of a level $I \sim 10^{-4}$ to 10^{-3}. The results are summarized in Table 1.

Apart from the large-scale anisotropy, several experiments showed that at the same energy scale smaller angular scale excesses and deficits do exist, with extensions from a few degrees in the sky up to about 20 deg in one direction (Abdo et al. 2009; Abbasi et al. 2011). Most recently, it was shown that the large-scale anisotropy which is present at TeV energies vanishes in the southern hemisphere at around 400 TeV and a new component emerges instead, a clear deficit of a 20 deg scale and with an intensity of the order of $\sim$10^{-4} (Abbasi et al. 2012). While the deficit has a significance of 6.3σ, a clear excess is not yet distinguishable from current statistics (Abbasi et al. 2012). This result was cross-checked with IceTop data. IceTop data show a slightly higher anisotropy level, but is generally consistent with the IceCube results. It could further be shown that the deficit is present up to an energy of 1 PeV (Aartsen et al. 2013). What is important about this result is that it is not necessarily a simple dipole component, which would just be symmetric in excess and deficit, but the anisotropies clearly display disjunct excesses and deficits. In the model presented here, a full dipole is only observed when the velocity field responsible for the anisotropy covers the entire mean free path region. As soon as a velocity field does not cover the entire 4π range anymore, the dipole structure would become a large-scale structure, spatially smaller than a dipole.

First, we may have to ask why we should expect isotropy of CRs at all. The essential answer was given by Schlüter & Biermann (1950): magnetic fields get strengthened until they scatter CRs into near perfect isotropy (also found by Hanasz et al. 2004, 2009). On this basis, they estimated the strength of magnetic fields to be of the order of 4 μG, an estimate that has held up remarkably well (e.g., Beck et al. 1996). Thus, we can expect isotropy in the reference frame of the local interstellar medium (ISM), which is very well coupled to the magnetic fields (e.g., Appenzeller 1974), a connection that is kept by instabilities (Parker 1966). However, the Sun was only coupled to the ISM at birth, 4.5 billion years ago: interaction with massive interstellar gas clouds slowly increases the peculiar velocity of stars with age (e.g., Julian 1967; Wielen 1975), and so at the age of stars like the Sun the increase in peculiar velocity is expected to be about 40 km s^{-1}, which is actually somewhat more than deduced from three-dimensional observations using the water maser spectral line, which gives radial motions, and very long baseline interferometry observations, which give sideways motion, vector, and relative positions (Reid et al. 2009). Therefore, within such a velocity the CR anisotropy should be small relative to the average ISM around the solar system.

In this paper, we discuss the possible origin of the large-scale structure anisotropies at $\sim$10 TeV with some comments on larger and smaller energies.

2. MODELING THE LARGE-SCALE ANISOTROPY WITH A LOCAL ISM STREAM

Here, we present the model of a local flow field which leads to a dipole anisotropy in the CR arrival direction. The flow field is created by an old supernova remnant (SNR) of an age around 100,000 yr or older: the hottest normal phase of the ISM is at about a density of 3×10^{-3} cm^{-3} and a temperature of about 4×10^6 K (Snowden et al. 1997; Hagihara et al. 2011), confirming earlier expectations (Lagage

Table 1
The Observed Large-scale CR Anisotropies

	IceCube		IceTop		Tibet	Milagro	SuperK
Refs	(1)	(2)	(3)	(3)	(4)	(5,6)	(4)
$\langle E \rangle$ (TeV)	20	400	400	1000	4–12	6	10
I (10^{-4})	8	4	16	31	4	4	7
Hemisphere	S	S	S	S	N	N	N
R.A. (deg)	50 d	90 m	90 m	90 m	65 d	190 d	35 d

Notes. The phase of the anisotropy is given, where d indicates the phase of the dipole and m indicates if only a minimum is present.
References. (1) Abbasi et al. 2010; (2) Abbasi et al. 2012; (3) Aartsen et al. 2013; (4) Amenomori et al. 2006; (5) Abdo et al. 2008; (6) Abdo et al. 2009.

& Cesarsky 1983). After a supernova explodes into the ISM, the expansion of the shock racing through the ISM is fast at first, accumulating evermore material from the ISM, and then slows down (Sedov 1958; Cox 1972) until the flow becomes subsonic and sub-Alfvénic; thereupon the flow coasts along, and basically gets slowly disorganized by mixing and encountering clouds. Gaensler et al. (2011) confirm that the typical sonic Mach number is low, of the order of two or less. At the density and temperature of this most tenuous phase, the signal speeds will thus be around 160 km s^{-1}. Thus, the velocity fields of the late evolution of SNRs will run at or a bit below these velocities, but later decay rather slowly. Cox & Smith (1974) state that the velocity of the gas should be larger than 10 km s^{-1} in general, which gives a velocity range of 10 km s$^{-1} < v <$ 160 km s^{-1}. The average density across all media in the 200 pc thick layer of the ISM is of the order of 1 cm^{-3} (Cox 2005). Using this average density, we obtain a velocity scale of the order of 100 km s^{-1} at a scale of about 30 pc, using the simple expressions of Cox (1972). The associated timescale is of the order of 2×10^{5} yr. Thus, the SNR is no longer supersonic or super-Alfvénic in the hot medium. Observational data on pulsar activity and their associated SNRs support the scale of 30 pc (Braun et al. 1989), and a timescale for the powering of 2×10^{4} yr, less than 2×10^{5} yr, so consistent with the numbers suggested here for the hot interstellar gas. The confinement time for CR particles in decaying SNRs has also been estimated to be relatively short, of the order of 10^{4} yr (Berezhko & Völk 2004), in agreement with the arguments by Braun et al. (1989). CRs will travel most easily in that phase of the ISM, where the Alfvén velocity is the highest, due to limiting the streaming instability at the Alfvén velocity. Therefore, we might expect the CR particles that we observe to come most effectively through this phase. However, as the observations show (Appenzeller 1974) the magnetic fields permeate the clouds, and so it is more suitable to use the average density of 1 cm^{-3}. So the old velocity field of SNRs having gone subsonic and sub-Alfvénic in the highest temperature medium corresponds to velocities of about 100 km s^{-1} and to length scales of about 30 pc.

Thus, if a supernova explosion happened in the Sun's vicinity some 100,000 yr ago, a flow field of around 100 km s^{-1} at a scale on the order of 30 pc would still exist, giving momentum to CR particles which could lead to a dipole anisotropy with an excess due to a coherent flow.

Item 1. Compared to the large-scale anisotropy prediction of the Compton–Getting effect, this prediction can result in, but does not require, a full dipole: if the velocity field covers the entire mean free path region, a full dipole is expected. With increasing energy, the mean free path becomes larger and thus the velocity field might not cover the entire region

anymore, leading to a large-scale anisotropy smaller than 4π. It is therefore expected that the scale of the anisotropy decreases with increasing energy, consistent with observations. Along with this, a slight decrease of the amplitude is expected, as fewer CRs will be affected by the velocity field. This decrease in amplitude should mainly be proportional to the fraction of CRs involved, ξ, which should roughly correspond to the size of the anisotropy region, $\xi \approx \Omega/2\pi$. This is well compatible with the observed decrease of angular size and intensity from 20 TeV to 400 TeV, as observed with IceCube (Abbasi et al. 2010, 2012). More detailed observations with IceTop are possible at several hundred TeV up to PeV energies and will be able to test this model. At this point, first results show a systematically larger anisotropy than IceCube at the same energy (400 TeV), which can be assigned to the relatively large statistic and systematic uncertainties (Aartsen et al. 2013).

2.1. The Model

We now consider CR particles diffusing through the ISM with a surface of last scattering, given by the mean free path of the diffusion. Figure 1 shows a schematic picture of the model presented here. It shows the region of last scattering and the inner region in which the particle is not deflected. Thus, the particles will be swept along with the flow. Considering the scattering of CRs arriving at Earth, at such a distance from us when they first point in our general direction, that surface can be called *the surface of last effective scattering*, one mean free path away. If that region has a general flow field, it will imprint an anisotropy upon the CRs coming to Earth. This does not necessarily need to be a full cosine angle dependence as would be the case for the standard Compton–Getting effect. Depending on the flow configuration, a partial sky coverage is present only, for instance, if the flow field does not fill the entire region within the surface of effective last scattering.

Using a diffusive description of CR propagation, Blasi & Amato (2012a, 2012b) have modeled the possible CR anisotropies, and have found that the anisotropy could be quite large. Here, we propose to take a slightly different route, comparing the influence of both diffusion and velocity fields, always emphasizing that the surface of last effective scattering is "thick": it is not infinitely thin, but has an extension ΔR due to the exponential path-length distribution $\lambda_{\mathrm{mfp}} \propto \Delta R$ as discussed by Garcia-Muñoz et al. (1987). Thus, the higher the energy, the larger the scale, but also the larger the smearing over all lower scale spatial variations. *Item 2a.* This implies that pitch-angle scattering from the turbulent magnetic field is included in the description of a thick surface of effective scattering: the surface of last scattering is itself as thick as the typical distance to it, so that the very concept includes the small amount of extra
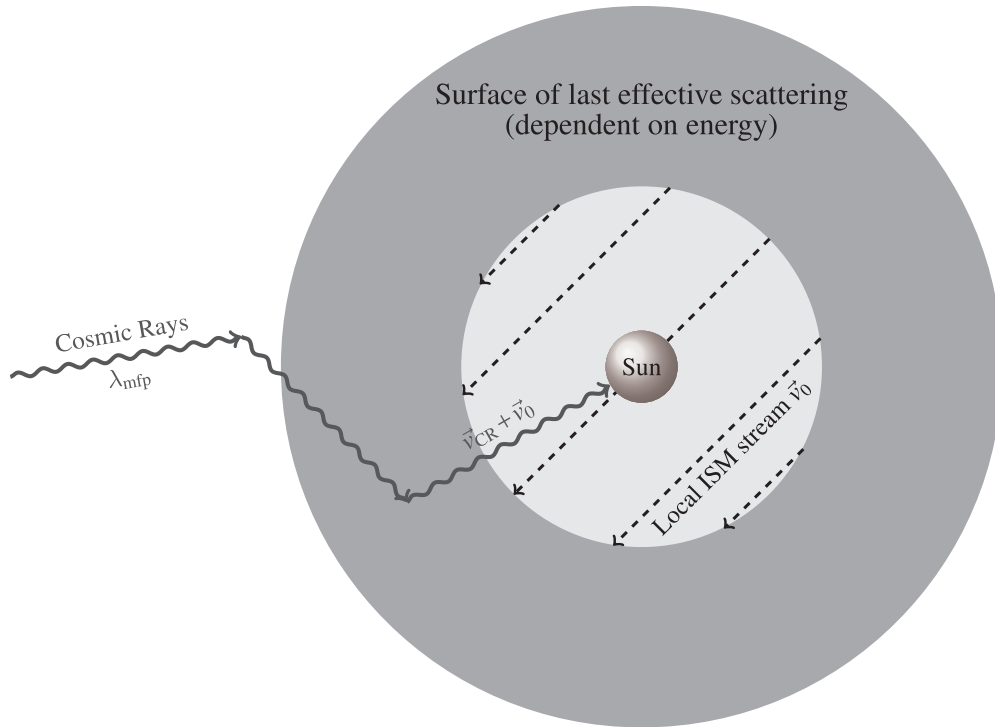
Figure 1. Schematic geometry of the surface of effective last scattering, shown for the special case where the path shown in projection is perpendicular to the direction of the regular magnetic field in the plane of the graph, in this specific example almost parallel to the flow; the helical motion is thus invisible in such a projection. *Item 2.* The thickness of the surface of last effective scattering is estimated to be of the same order as the mean free path, due to pitch-angle scattering from the turbulent magnetic field (see the text for further discussion).

scattering that does occur close to us. The net effect is that small angular scales are smeared out, but on the larger scales the amplitude is only weakly reduced. From the surface of last effective scattering, CRs will still scatter a small amount smearing out the small angular scales; that is why we address only large angular features in this paper. In Beck et al. (1996), it is stated that in our Galaxy the irregular field component is of the order of half the total magnetic field strength, with a relatively large uncertainty, so a large-scale prevailing field is plausible to assume. Beck et al. (1996) also note that the sky as seen in rotation measure (RM) values exhibits large angular coherent patterns, supporting such an interpretation. Finally, they note that in other disk galaxies, similarly, large-scale coherent patterns in RM maps have been discerned, again supporting such an interpretation.

Item 2b. Magnetic fields can be thought of a messy twisted and braided set of flux tubes (e.g., Jokipii & Parker 1969), as for instance, apparently observed in vertical radio filaments near the Galactic center (Yusef-Zadeh & Morris 1987). The ISM in a differentially rotating galaxy with vertical chaotic motions due to, e.g., the Parker instability (Parker 1966) can be thought of as such a mixture of flux tubes. Such mixing then also leads to reconnection (e.g., Lazarian et al. 2012). It follows that CRs can switch around between such flux tubes, thus connecting any given system such as the Earth to a large solid angle from which CRs can be received given a distance scale of the order of the surface of last effective scattering; over such a distance scale the solid angle can then be of the order of unity.

The escape from the Galactic disk can be described as a random walk with the step size a function of energy (Chandrasekhar 1943). Another related description is with the exponential path-length distribution (Garcia-Muñoz et al. 1987). The escape time from the thick Galactic disk (Beuermann et al. 1985; Ferrando 1993; Brunetti & Codino 2000) of an approximate half-thickness

of $d = 1$–2 kpc is of the order of 10^7 yr, and using the argument above depends on energy as $E^{-1/3}$. Considering a possible heavy composition of Galactic CRs at $10^{18.5}$ eV, we will scale to proton energies at 10^{17} eV. Under the cautious assumption that the thickness H is of order three times the mean free path at the maximal energy, we obtain a mean free path $\lambda_{\rm mfp}$ of the order of

$$\lambda_{\rm mfp} = \frac{1}{3} H \left(\frac{E}{10^{17}\,{\rm eV}} \right)^{1/3} \simeq 10^{18.5} \left(\frac{E}{\rm GeV} \right)^{1/3} {\rm cm}. \quad (1)$$

Since at that level in vertical direction, about 1–2 kpc, we have a transition to a Galactic magnetic wind (Everett et al. 2008, 2010; Everett & Zweibel 2011), which also scatters particles quite effectively due to the larger scale and the $1/r$-behavior of the magnetic field (Parker 1958; Biermann & de Souza 2012), this ought to be enough to ensure near isotropy. The scale of the order of 20 pc is then reached for particle energies of about 10 TeV with an energy dependence as $E^{1/3}$, and a scale of the order of 70 pc is reached at about 400 TeV. Thus, the flow field of an old SNR would produce a dipole anisotropy for particles at around 10 TeV energies if the field is fully coherent. At scales where the field starts to become incoherent, the dipole will weaken and be replaced by lower level anisotropies due to smearing.

The intensity of the dipole anisotropy can be determined as follows: following arguments first presented by Compton & Getting (1935), a flow field of velocity v with a pitch angle α toward the regular magnetic field produces an anisotropy level ΔI of

$$\frac{\Delta I}{I_{\rm av}} = \frac{v}{c} (p + 2) \langle \cos \alpha \rangle, \quad (2)$$

with respect to the average intensity $I_{\rm av}$. Here, p is the spectral index of the incoming particle spectrum $dN = E^{-p} dE$. Here,

the observed CR flux below the knee gives $p \approx 2.7$. For velocities of a flow field component parallel to the magnetic field of $v \cdot \langle \cos \alpha \rangle \sim 50$ km s^{-1} on average, the expected anisotropy level would correspond to

$$\frac{\Delta I}{I_{\mathrm{av}}} \approx 8 \times 10^{-4} \cdot \left(\frac{v}{100\,\mathrm{km\,s^{-1}}} \right). \qquad (3)$$

This corresponds to the observed intensity level within experimental error bars and allows for flow field velocities of the order of 100 km s^{-1} if the average pitch-angle distribution is of the order of $\langle \cos \alpha \rangle \sim 0.5$. The latter value is of course not known, but as long as there is a significant velocity component parallel to the regular magnetic field, the experimental results can be explained as an effect of this model.

2.2. Discussion

While we will discuss possible uncertainties in the numbers presented above in the next section, we note subtleties of the model that are negligible at this point.

Position of the SNR center. It has to be noted that the effect described above does not require the SNR to be centered on the Sun's position: the effect is there as soon as we have coherent motion at the surface of last scattering over about one radian in one direction laterally, and in depth by about the distance itself, so $\Delta r / r \sim 1$; consistent with this the data suggest an effect that varies across the sky. Massive stars that later produce supernovae form in the cold disk which is only of the order of 200 pc full width (Cox & Smith 1974; Cox 2005). Using the timescale from above of about 200,000 yr yields a length scale about a factor of two larger, with the energetics adopted by Cox (1972). The irregular flow field will be dominated by a single most recent supernova up to this scale combined with several supernovae that are somewhat older. Above, we show that the anisotropy level is expected to be on the order of $\sim 10^{-3.6}$, so in agreement with Blasi & Amato (2012a, 2012b) not completely negligible compared to the influence of the flow itself. Also, just like the flow, the directionality is not isotropic; the only key difference is that the source contribution can only be positive, but the modified Compton–Getting effect can be either positive or negative; the observations suggest at 400 TeV that the major effect is a deficit, consistent with a modified Compton–Getting effect.

Measurements of the ISM. While measurements of the ISM do exist up to scales of ~ 100 pc (e.g., Lallement et al. 2003; Redfield & Linsky 2002, 2004), these are sensitive to cold, molecular gas. Here, we consider a flow velocity in the hot ISM at low densities, i.e., $\rho \sim 10^{-2.5}$ cm^{-3}. Therefore, there is no direct measurement confirming or rejecting a local flow at this point. The same is true for the orientation of the orientation local magnetic field up to a scale of 100 pc.

Effects of the gyroradius. CRs scatter on irregularities of the magnetic field, and so in addition to their steady gyrating motion, they slowly change their pitch angle and also move slowly sideways from gyrating around one field line to the next (e.g., Drury 1983; Jokipii 1987). Thus their arrival direction at Earth is completely dominated by these effects. Given a source of CRs at some distance, the arrival direction at Earth of CRs from such a source is highly irregular and becomes completely isotropic for distances larger than λ_{mfp}:

$$\lambda_{\mathrm{mfp}} = \frac{pc}{ZeB} \frac{B^2/(8\pi)}{I(k)k}, \qquad (4)$$

where the first term is the Larmor radius $r_g = pc(ZeB)$ of a charged particle of momentum p and charge Ze, while the second term is the ratio of the energy densities of the regular magnetic field B and the irregular magnetic field in resonance with the Larmor motion at wave number k with $k = (2\pi)/r_g$. This formula is valid for quasi-linear behavior, which means that each scattering event is small compared to the Larmor gyrating motion. We can call the surface at that distance the surface of last effective scattering; we note from the data on transport (e.g., Garcia-Muñoz et al. 1987), which show that an exponential path-length distribution describes the interaction data very well, that the spread in the mean free path is the same length again.

So CRs from some source closer than that mean free path leave an anisotropic imprint in their arrival directions, and sources at that distance or larger arrive isotropically.

Thus, if there are systematic effects at the surface of last effective scattering, then they leave an imprint on the arrival directions. Systematic motions are such effects, since—if they were systematic over all sky—they leave a dipole imprint. Therefore, such systematic motions should remain visible as systematic deviations from isotropy, just like the motion of the solar system through the local reference frame of CRs (Compton & Getting 1935), which is a dipole effect. If, on the other hand, the systematic motions pertain only to part of the solid angle spanning the surface of last effective scattering, the minimum solid angle is equivalent to the uncertainty itself, so about 60 deg (one radian) or more.

2.3. Summary

We conclude that old SNRs leave traces of their flow field for much longer times than traces of their individual CR contribution. Therefore, the population of CR particles in its scattering is more strongly influenced by these flow fields than by the inhomogeneity of the sources in space and time, unless the source is unusually young. The anisotropy given by the flow fields is usually not dipole-like, since looking into different directions in the sky will see the thick surface of last effective scattering usually in different old SNR flow fields.

It follows that there is an optimum particle energy to detect anisotropies, and at any larger energies we begin to smooth over several irregular flow patches (which clearly shows that the diffusion approximation is no longer adequate in describing anisotropies), so that the anisotropies become smaller. Also, going to significant larger scales we begin to see different flow patches, and so the directionality would become uncorrelated at larger energies and thus larger scales as seen by inverting the scale energy connection: $E \sim \lambda_{\mathrm{mfp}}^3$; this is derived by inverting the Kolmogorov spectrum with the exponent 1/3. The IceCube data are consistent with both these effects, as the anisotropy is weaker at higher energies, and also uncorrelated in direction. Finally, we note that of course the Sun may have a peculiar velocity with respect to its environment: this has been shown by very long baseline interferometry observations to be a small effect, 10–20 km s^{-1} (Reid et al. 2009). However, we need to emphasize that the uncertainties are large in such simple arguments. Thus, we need to match particle energy and expected SNR scale: the old SNRs of about 30 pc match the mean free path for about 10 TeV. This should then correspond roughly to the maximum of any anisotropy; at larger spatial scales and thus larger energies the anisotropy is smeared out across several old SNRs; at lower energies we reach portions of an old SNR, not giving the full amplitude. Another important aspect is that in this model there is no expectation of symmetry, since in one

The Astrophysical Journal, 768:124 (8pp), 2013 May 10

Biermann et al.

direction and the directly opposite direction the surface of last effective scattering will touch different old SNRs.

However, how does this compare to the elaborate calculations of Blasi & Amato (2012a, 2012b)? These authors use the diffusion approximation, which of course begins to fail when the scale of the inhomogeneities becomes similar to the scale of the mean free path of scattering itself, a case which we argue we have here. So, using the diffusion approximation increases the apparent anisotropy when the scale of old SNRs is reached, while treating the scattering directly it becomes obvious that then the "thickness" of the surface of last effective scattering itself begins to smear out anisotropies and so decreases it.

Another aspect is that counting nearby sources of CRs, when old SNRs do not only produce a flow field, but also slowly disperse the CRs as a function of time, produces a gradient in CRs, which would also give an anisotropy; however, the data suggest that the aspect is a significant deficit, but not a significant excess (Abbasi et al. 2012), and this is more easily explained as a Compton–Getting effect (Compton & Getting 1935), which can have either sign but does not have to be symmetric, as noted above.

A key assumption in this model is the use of a Kolmogorov spectrum for the irregularities across the entire energy range of Galactic CRs, from 10^9 eV to 10^{18} eV, a point on which we agree with Blasi & Amato (2012a, 2012b). Only this assumption allows the match in length scales.

The amplitude at around 10 TeV would then be of the order of three times what is seen for the motion of the Earth around the Sun, so about 10^{-3} at most, and would correspond to angular scales of about 60 deg. At larger energies the anisotropies begin to get smeared out. This is consistent with what is observed.

3. DISCUSSION OF ASSUMPTIONS AND UNCERTAINTIES

In this section, we first discuss other evidence about the scattering of CRs, such as the energy dependence of transport, spallation, and comparing electrons and nuclei. Assuming Kolmogorov-like turbulence, the energy behavior of the mean free path for CR scattering with magnetic field turbulence is expected to be $E^{1/3}$, as also stated in Equation (1). If the turbulence model is changed, this energy dependence might change as well. A test of the energy dependence of the mean free path is the investigation of spallation products. It is well known that at the same time as particles scatter around they also interact, and so the spectrum of the spallation secondaries, like Boron, compared with Carbon, should also reflect a similar energy dependence. The observed B/C ratio scales as $E^{-0.54}$ (Ptuskin 1999), which is steeper than what is expected for a Kolmogorov spectrum. While it could be consistent with a Kraichnan spectrum $k^{-3/2}$ (Kraichnan 1965), Kraichnan turbulence implies a lower dimensionality due to a dominant magnetic field. This is not given in the ISM as discussed by Beck et al. (1996). The contradiction can be resolved: the massive stars, which produce most of the CR Carbon before they explode, are Wolf–Rayet stars. These stars have a powerful wind and eject most of their zero-age main-sequence mass into the wind before they explode (Prantzos 1984). This wind forces most of the stellar mass as well as a large amount of ISM material into a thick shell. Therefore, at the time of the explosion, typically more than half of the original stellar mass is contained in the wind and its shocked shell, composed of old stellar and ISM material. There, the CRs excite a spectrum of magnetic turbulence (Bell 1978a, 1978b). This is only done in the environment of the SNR
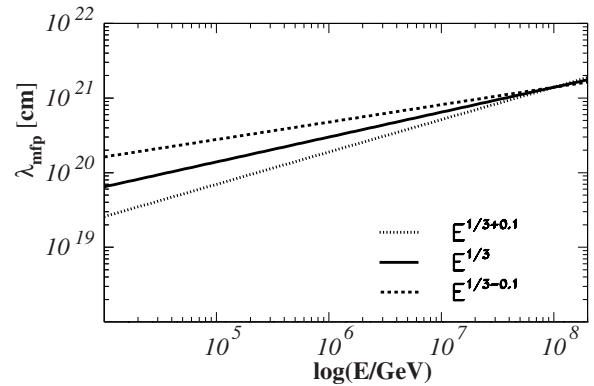
Figure 2. Dependence of the mean free path on the energy dependence of the mean free path, depending on the underlying turbulence model.

and this scenario does not apply to the transport through the Galaxy. Biermann (1998) calculated the energy dependence of the escape yielding for the B/C ratio an energy dependence of $E^{-5/9}$ based on the excitation of the irregularities by the CRs (Bell 1978a, 1978b) is fully consistent with the observed spectral dependence (Ptuskin 1999). This suggests that most of the hadronic particle interactions happen in these shells. A recent example of observing CR interactions with matter directly in γ-ray data was shown by Berezhko et al. (2009), who argued directly for interaction in a wind environment. It also implies that there is a minimum interaction, or in other words, a finite minimum path length of interaction, stemming from the fact that the particles at very high energies do not scatter through the wind shell, but instead convect (Biermann 1993; Biermann et al. 2001; Nath et al. 2012). In this latter point of a finite residual path length, the model is consistent with the results by the Tracer experiment (Obermeier 2011), but requires more statistical data for final confirmation. There is another test for this argument from a comparison of the electron and proton spectra, which should have the same injection slope at TeV energies if arising from the same shock mechanism in the same source class; at energies well above 10 GeV the CR electrons have a spectrum of $E^{-3.26\pm0.06}$ up to TeV energies (Wiebel-Sooth & Biermann 1999) and clearly have been steepened by synchrotron and inverse Compton losses (Kardashev 1962), and so their injection spectrum is $E^{-2.26\pm0.06}$. Comparing this with the CR protons (CREAM: Yoon et al. 2011), which give a spectrum of about $E^{-2.66\pm0.02}$ near TeV energies, the difference to the corrected CR electron spectrum gives the energy dependence of the diffusive escape, $E^{-0.40\pm0.06}$, fully consistent with a Kolmogorov law. A spectrum of close to $E^{-8/3}$ matches the prediction for wind-supernova CRs (see also Biermann et al. 2010b on the match to the new CREAM data; Yoon et al. 2011). On the other hand, the arguments for the positron fraction rising with energy (Biermann et al. 2009) support the point of view that wind supernovae are more important for observed CR electrons at these energies; the predicted ratio of CR positrons to CR electrons (Biermann et al. 2009) has recently been confirmed again by Ackermann et al. (2012). Therefore, in the following we will use the concept that for ISM propagation the relevant spectrum of irregularities has a Kolmogorov-type spectrum. We conclude that the energy dependence of transport, spallation, and comparison of CR electrons and CR nuclei can all be consistently explained. All the previous arguments are used here for the CR energies for which anisotropies have been observed.

Figure 2 shows the uncertainties from the energy dependence, allowing for a variation in the exponent of ±0.1, so $E^{1/3\pm0.1}$.

5

Since the mean free path can be estimated at 10^{17} eV, where CRs escape the Galaxy, from extrapolating to the relevant energy scale of 10 TeV, the mean free path is determined as $\lambda_{\mathrm{mfp}}(E = 10\,\mathrm{TeV}) = 10^{19.81\pm0.3}$ cm. This allows for distance scales between 10 and 21 pc, where the lower mean free path limit implies strong evolution with energy. Concerning the anisotropy at 10 TeV, this is well compatible. Given the fact that the anisotropy changes toward higher energies, i.e., at 400 TeV and above, the SNR flow field cannot be dominant anymore. This then concerns distance scales between 35 and 70 pc, implying that the supernova flow field cannot be more extended than ~35 pc.

The calculation also relies on the assumption that the CR distribution arriving at the surface of last scattering is isotropic. For turbulence models in magnetic clouds resulting in an anisotropic distribution of CRs, the flow velocity of the CRs is influenced and the resulting anisotropy will not correspond to a dipole feature anymore. At this point, there is no evidence in the data for anisotropic scattering, so we consider this assumption as reasonable.

The level of anisotropy is directly determined by the velocity of the flow field. Measurements indicate a level of anisotropy corresponding to $\Delta I/I_{\mathrm{av}} \sim 10^{-4}$ to 10^{-3} within experimental uncertainties (see Table 1). This is consistent with velocities of 12.5 km s$^{-1} < v < 125$ km s^{-1} (see Equation (3)). Within the uncertainty of the SNR flow field, those numbers are fully consistent with the expectations (see Section 2).

4. OTHER APPROACHES TO MODEL THE ANISOTROPY

Since the anisotropy at TeV energies was first detected in 2005, different models have been developed to explain the observed features. Here, we shortly discuss the different models in the light of recent data.

4.1. Sources

The first effect is an overall gradient of CR particles in a disk galaxy like ours (Ginzburg & Syrovatskii 1964); however, a disk galaxy is usually a spiral, with some variation across the spiral arms (e.g., Beck & Hoernes 1996), so that the key radial gradient has to be considered along the spiral arms, effectively increasing the radial scale of comparison by $\{\cos\theta\}^{-1}$, where θ is the angle of the spiral arms with respect to a circle. This implies that we expect anisotropy of the order of 0.1% by dividing 20 pc by several times 8 kpc, but symmetric, which is not seen in the data. This probably implies that this effect is washed out by other influences. Detailed observations at several wavelengths in radio and infrared clearly show (e.g., Tabatabaei et al. 2007) that the local variations on scales of a few tens of pc and larger dominate the unevenness of the non-thermal radio emission, and probably also of the CR distribution. At much higher energies this effect may have been detected (see, e.g., Teshima et al. 2001), but even there source regions may dominate what is seen.

The second effect is due to the diffusion straight out from the disk into the halo Galactic magnetic wind (Everett et al. 2008, 2010; Everett & Zweibel 2011). However, this effect is of second order due to the symmetry, and depends critically on where the mid-plane is for this flow and diffusion, which we do not know. For the lack of a better number, assuming the distance from Earth to the mid-plane of the flow field to be about 40 pc, and the vertical scale of the flow to be 1.5 kpc suggests an asymmetry of the order of 6×10^{-4}, no longer visible at

any length even approaching 40 pc. This again is clearly not dominant in what we observe.

Finally, the obvious most recent source, an idea that has been explored very many times (e.g., Völk et al. 1988; Teshima et al. 2001; Erlykin & Wolfendale 2006; Yüksel et al. 2009). It is clear that statistically there must be a most recent source within any given distance range. The question is, what is its signature? The supernova rate in our Galaxy has been estimated to be of the order of one per 30 yr, with an uncertainty toward longer times of a factor of three (see, e.g., Biermann & Cassinelli 1993; Biermann et al. 1995); averaging this uncertainty suggests that one supernova in 50 yr, to within a factor of two is also compatible with the number derived by Diehl et al. (2006). The probability to then have a supernova explode within a certain radial distance over a certain time, at our distance from the Galactic center, can then be estimated. Since the supernova rate is reduced at our distance from the Galactic center with respect to the average can be crudely estimated to be of the order of three, so that in our part of the Galaxy the supernova rate may be about one in 150 yr. It follows that within a distance of $r = R_{1.3}$ 20 pc from us the timescale between supernovae is of the order of $10^{7.6} R_{1.3}^{-2}$ yr.

This, then, allows us to derive the diffusion coefficient derived above as $10^{29.8}$ cm^2 s^{-1} at 10 TeV; this is slightly larger than the estimate given by Blasi & Amato (2012a, 2012b), who use a different concept of CR propagation, but our number is close to older estimates. The uncertainties are dominated by systematics, since different lines of reasoning have been used to derive the coefficient as well as its energy dependence.

This implies that over a distance of 20 pc the diffusive timescale is of the order of $10^{2.4} R_{1.3}^{2}$ yr. Therefore, the dispersion of any original cloud of CR particles is extremely effective, with the typical timescale between supernovae taken from above we obtain a radial range of many kpc numerically, and a dilution relative to the average CR energy density of about $10^{-5.4}$, so the typical anisotropy expected from supernovae should be quite small. This predicted anisotropy scales with the reference distance as $R_{1.3}^{+3}$, so for a mean free path at 10 TeV larger by a factor of two, well within the uncertainties, we obtain a predicted CR anisotropy of $10^{-4.5}$, getting close to numbers observed. This clearly implies that a recent supernova explosion cannot be immediately discounted as a contributing origin for CR anisotropies, confirming, e.g., Völk et al. (1988), Teshima et al. (2001), Erlykin & Wolfendale (2006), Yüksel et al. (2009), and others.

4.2. Magnetic Field Isotropy?

There are several other effects that need to be considered in the propagation of CRs. First of all, the spectrum of irregularities may be well approximated by an isotropic Kolmogorov spectrum, but since the observed magnetic field distribution is never completely irregular (Beck et al. 1996) there can always be effects from this underlying anisotropy. Furthermore, even the irregularities themselves are never perfectly isotropic either (e.g., Malkov et al. 2010; Lazarian & Desiati 2010; Desiati & Lazarian 2013), and so such an assumption has to be taken with great caution, even though it may appear that it works relatively well. Finally, and perhaps most importantly, the history of recent supernova explosions in the solar neighborhood will give an imprint of irregularity from the source distribution; however, since the time to escape is much larger than the time to replenish the CR population this should perhaps not be dominant until one gets to really high energies.

Also, extreme scattering events of radio waves suggest the presence of very small high electron density screens in the ISM (Fiedler et al. 1987; Bignall et al. 2003; Lovell et al. 2008). However, the sizes of the screens inferred from the data do not suggest that they dominate the ISM.

The sky maps in radio rotation measure (Oppermann et al. 2012), in radio emission (Berkhuijsen et al. 1971), and other wavelengths usually integrate over much larger distances that it is difficult to be sure of a correlation with the detected anisotropies. There may be a correlation of some radio features like *Spur 185−* (Berkhuijsen et al. 1971) with features in Tibet, Milagro, SuperK, and IceCube data; there may be a correlation with *Loop I* in IceCube data, and *Loop IV* in Tibet data; and finally, there may be a correlation with *Spur 195+* in Milagro data. The deficit in the IceCube flux at 20 TeV is remarkably close to the center of *Loop I*. It needs, however, a careful analysis of the CR data and a detailed modeling of the theory in order to investigate the causality of the signatures; today's radio data are much better (e.g., Oppermann et al. 2012; van Eck et al. 2011; Pshirkov 2011), but we need yet more significant CR data.

After subtracting the large angle features it is possible to identify small angular scale features (Abdo et al. 2008), which may be related to solar wind effects such as the heliotail (Nagashima et al. 1998; Drury & Aharonian 2008; Lazarian & Desiati 2010; Desiati & Lazarian 2013), or nearby stars like Aldebaran (van Leeuwen & Evans 1998), or even nearly extinct pulsar tails (e.g., Romanova et al. 2005). *IBEX* data (McComas et al. 2009, 2011) show that the solar wind interacts with the ISM and emits a steady stream of low-energy neutral atoms, producing a ribbon in the sky completely unanticipated by theory and earlier observations. Here, we do not address these small-scale features but focus on the explanation of the large-scale anisotropy.

It has been argued that we sit in a local bubble, the walls of which are made up of various old SNR shells. However, a detailed study (Mebold et al. 1998) suggests that this apparent bubble is not a coherent figure, but rather a motley assembly of filaments, clouds, and shells, assembled into a bubble only in perception. These features represent the local history of star formation, H II regions, the effect of other stellar activity, and old violent supernovae.

5. POSSIBLE TESTS FOR THE PROPOSED MODEL

There are several options to test this hypothesis with improved data.

The flow field. Measurements of the velocity field of the ISM up to distance scales of 100 pc are so far only possible for molecular gas. What is considered here, however, is the hot component of the gas with a low density of $\sim 10^{-2.5}$ cm^{-3}. In order to measure this component, UV or X-ray spectroscopic measurements could help in the future.

Turbulence model. We assume that an energy dependence of the mean free path for CR propagation is consistent with a Kolmogorov spectrum. This is consistent with current data. Further tests if the hypothesis holds would be a better energy resolution of the data sets for the anisotropy measurements. So far, data are available with median energies of around 10 TeV, 400 TeV, and 1 PeV. An unfolding of the energy spectrum would be necessary in order to confirm the exact behavior of the energy dependence. This would be an opportunity to have an independent measurement of the energy dependence of the scattering mean free path.

6. SUMMARY AND CONCLUSION

CR particles are believed to be injected into the ISM by supernova explosions as soon as their shocks slow down sufficiently to release the population of energetic particles; this may happen for progenitor stars of modest mass as explosions directly into the ISM or for very massive stars as explosions into their stellar winds. The distinction between these two types of supernova explosions (Stanev et al. 1993; Nath et al. 2012 and earlier papers) allows us to interpret the CR positron and electron enhancements (Biermann et al. 2009), the *Wilkinson Microwave Anisotropy Probe* haze of high-frequency radio emission as well as the 511 keV annihilation line near the Galactic center (Biermann et al. 2010a), as well as the upturn in the CR spectra of nuclei (Biermann et al. 2010b). Finally, it allows us to understand the KASCADE–Grande spectra of CR particles at energies beyond 10^{15} eV (Biermann & de Souza 2012), as well as allowing us to use the CR particles as injection seeds for the ultra-high-energy CRs (Gopal-Krishna et al. 2010; Biermann & de Souza 2012). Considering the explosion of stars into their stellar winds as elaborated above to explain the spallation energy dependence as a process in loco allows then the ensuing transport through the ISM to be consistent with a Kolmogorov irregularity spectrum (e.g., Kolmogorov 1941; Sagdeev 1979; Goldstein et al. 1995). This has been shown to be consistent with observations (Spangler & Gwinn 1990), which in turn has been demonstrated to be consistent with the low level of anisotropies (e.g., Biermann 1993; Blasi & Amato 2012a, 2012b).

In this paper, we suggest that the observed dipole anisotropy is due to a modified Compton–Getting effect. This is due to the magnetized flow field of old slowly disappearing SNRs and would give rather large angle scale fluctuations, since the mean free path is valid in all spatial directions, and so angular scales, as noted above, should be of the order of 60 deg. The effect is a sum of uncorrelated monopole components. That feature distinguishes this proposal from most other possibilities, which can easily produce small scales. A key assumption is that CRs are scattered isotropically and thus—without any extra velocity field—arrive with an isotropic distribution of particles in phase space at the surface of last scattering as described above.

The effect suggested here predicts that at energies apart by more than an order of magnitude the anisotropies should become uncorrelated, unless we sit in a very large scale substantial flow field. Averaging over several typical old SNR scales the anisotropies should decrease with energy. Finally, to first order the anisotropies near about 10 TeV should have angular scales of the order of 60 deg.

REFERENCES

Aartsen, M. G., Abbasi, R., Abdou, Y., et al. 2013, ApJ, 765, 55
Abbasi, R., Abdou, Y., Abu-Zayyad, T., et al. 2010, ApJL, 718, L194
Abbasi, R., Abdou, Y., Abu-Zayyad, T., et al. 2011, PhRvD, 83, 012001
Abbasi, R., Abdou, Y., Abu-Zayyad, T., et al. 2012, ApJ, 746, 33
Abdo, A. A., Allen, B., Aune, T., et al. 2008, PhRvL, 101, 221101
Abdo, A. A., Allen, B. T., Aune, T., et al. 2009, ApJ, 698, 2121
Ackermann, M., Ajello, M., Allafort, A., et al. 2012, PhRvL, 108, 011103
Amenomori, M., Ayabe, S., Bi, X. J., et al. 2006, Sci, 314, 439
Appenzeller, I. 1974, A&A, 36, 99
Beck, R., Brandenburg, A., Moss, D., Shukurov, A., & Sokoloff, D. 1996, ARA&A, 34, 155
Beck, R., & Hoernes, P. 1996, Natur, 379, 47
Bell, A. R. 1978a, MNRAS, 182, 147
Bell, A. R. 1978b, MNRAS, 182, 443
Berezhko, E. G., Pühlhofer, G. P., & Völk, H. J. 2009, A&A, 505, 641
Berezhko, E. G., & Völk, H. J. 2004, ApJ, 611, 12
Berkhuijsen, E. M., Haslam, C. G. T., & Salter, C. J. 1971, A&A, 14, 252
Beuermann, K., Kanbach, G., & Berkhuijsen, E. M. 1985, A&A, 153, 17
Biermann, P. L. 1993, A&A, 271, 649
Biermann, P. L. 1998, in Proc. Invited Lecture at the Nuclear Astrophysics Meeting at Hirschegg, Cosmic Ray Interactions in the Galaxy, ed. M. Buballa (Darmstadt: GSI), 211
Biermann, P. L., Becker, J. K., Caceres, G., et al. 2010a, ApJL, 710, L53
Biermann, P. L., Becker, J. K., Dreyer, J., et al. 2010b, ApJ, 725, 184
Biermann, P. L., Becker, J. K., Meli, A., et al. 2009, PhRvL, 103, 061101
Biermann, P. L., & Cassinelli, J. P. 1993, A&A, 277, 691
Biermann, P. L., & de Souza, V. 2012, ApJ, 746, 72
Biermann, P. L., Gaisser, T. K., & Stanev, T. 1995, PhRvD, 51, 3450
Biermann, P. L., Langer, N., Seo, E.-S., & Stanev, T. 2001, A&A, 369, 269
Bignall, H. E., Jauncey, D. L., Lovell, J. E. J., et al. 2003, ApJ, 585, 653
Blasi, P., & Amato, E. 2012a, JCAP, 01, 010
Blasi, P., & Amato, E. 2012b, JCAP, 01, 011
Braun, R., Goss, W. M., & Lyne, A. G. 1989, ApJ, 340, 355
Brunetti, M. T., & Codino, A. 2000, ApJ, 528, 789
Chandrasekhar, S. 1943, RvMP, 15, 1
Compton, A. H., & Getting, I. A. 1935, PhRv, 47, 817
Cox, D. P. 1972, ApJ, 178, 159
Cox, D. P. 2005, ARA&A, 43, 337
Cox, D. P., & Smith, B. W. 1974, ApJL, 189, L105
Desiati, P., & Lazarian, A. 2013, ApJ, 762, 44
Diehl, R., Halloin, H., Kretschmer, K., et al. 2006, Natur, 439, 45
Drury, L. O'C. 1983, RPPh, 46, 973
Drury, L. O'C., & Aharonian, F. A. 2008, APh, 29, 420
Erlykin, A. D., & Wolfendale, A. W. 2006, APh, 25, 183
Everett, J. E., Schiller, Q. G., & Zweibel, E. G. 2010, ApJ, 711, 13
Everett, J. E., & Zweibel, E. G. 2011, ApJ, 739, 60
Everett, J. E., Zweibel, E. G., Benjamin, R. A., et al. 2008, ApJ, 674, 258
Ferrando, P. 1993, in Proc. 23rd ICRC, ed. R. B. Hicks, D. A. Leahy, & D. Venkatesan (River Edge, NJ: World Scientific), 279
Fiedler, R. L., Waltman, E. B., Spencer, J. H., et al. 1987, ApJS, 65, 319
Gaensler, B. M., Haverkorn, M., Burkhart, B., et al. 2011, Natur, 478, 214
Garcia-Muñoz, M., Simpson, J. A., Guzik, T. G., Wefel, J. P., & Margolis, S. H. 1987, ApJS, 64, 269
Ginzburg, V. L., & Syrovatskii, S. I. 1964, The Origin of Cosmic Rays (Oxford: Pergamon; origin Russian 1963)
Goldstein, M. L., Roberts, D. A., & Matthaeus, W. H. 1995, ARA&A, 33, 283
Gopal-Krishna, Biermann, P. L., de Souza, V., & Wiita, P. J. 2010, ApJL, 720, L155

Guillian, G., Hosaka, J., Ishihara, K., et al. 2007, PhRvD, 75, 062003
Hagihara, T., Yamasaki, N. Y., Mitsuda, K., et al. 2011, PASJ, 63, 889
Hanasz, M., Kowal, G., Otmianowska-Mazur, K., & Lesch, H. 2004, ApJL, 605, L33
Hanasz, M., Otmianowska-Mazur, K., Kowal, G., & Lesch, H. 2009, A&A, 498, 335
Jokipii, J. R. 1987, ApJ, 313, 842
Jokipii, J. R., & Parker, E. N. 1969, ApJ, 155, 777
Julian, W. H. 1967, ApJ, 148, 175
Kardashev, N. S. 1962, AZh, 39, 393
Kolmogorov, A. 1941, DoSSR, 30, 301
Kraichnan, R. H. 1965, PhFl, 8, 1385
Lagage, P. O., & Cesarsky, C. J. 1983, A&A, 125, 249
Lallement, R., Welsh, B. Y., Vergely, J. L., Crifo, F., & Sfeir, D. 2003, A&A, 411, 447
Lazarian, A., & Desiati, P. 2010, ApJ, 722, 188
Lazarian, A., Eyink, G. L., & Vishniac, E. T. 2012, PhPl, 19, 012105
Lovell, J. E. J., Rickett, B. J., Macquart, J.-P., et al. 2008, ApJ, 689, 108
Malkov, M. A., Diamond, P. H., Drury, L. O'C., & Sagdeev, R. Z. 2010, ApJ, 721, 750
McComas, D. J., Allegrini, F., Bochsler, P., et al. 2009, Sci, 326, 959
McComas, D. J., Funsten, H. O., Fuselier, S. A., et al. 2011, GeoRL, 38, L18101
Mebold, U., Kerp, J., & Kalberla, P. M. W. 1998, in Proc. IAU Colloq. 166, The Local Bubble and Beyond, ed. D. Breitschwerdt, M. J. Freyberg, & J. Trümper (Berlin: Springer), 199
Nagashima, K., Fujimoto, K., & Jacklyn, R. M. 1998, JGR, 103, 17429
Nath, B. B., Gupta, N., & Biermann, P. L. 2012, MNRAS, 425, L86
Obermeier, A. 2011, PhD thesis, Radboud Univ. Nijmegen
Oppermann, N., Junklewitz, H., Robbers, G., et al. 2012, A&A, 542, A93
Parker, E. N. 1958, ApJ, 128, 664
Parker, E. N. 1966, ApJ, 145, 811
Prantzos, N. 1984, AdSR, 4, 109
Pshirkov, M. S. 2011, ApJ, 738, 192
Ptuskin, V. 1999, in Proc. ICRC, Vol. 4, ed. D. Kieda, M. Salamon, & B. Dingus (Melville, NY: AIP), 291
Redfield, S., & Linsky, J. L. 2002, ApJS, 139, 439
Redfield, S., & Linsky, J. L. 2004, ApJ, 602, 776
Reid, M. J., Menten, K. M., Zheng, X. W., et al. 2009, ApJ, 700, 137
Romanova, M. M., Chulsky, G. A., & Lovelace, R. V. E. 2005, ApJ, 630, 1020
Sagdeev, R. Z. 1979, RvMP, 51, 1
Schlüter, A., & Biermann, L. 1950, ZNatA, 5, 237
Sedov, L. I. 1958, RvMP, 30, 1077
Snowden, S. L., Egger, R., Freyberg, M. J., et al. 1997, ApJ, 485, 125
Spangler, S. R., & Gwinn, C. R. 1990, ApJL, 353, L29
Stanev, T., Biermann, P. L., & Gaisser, T. K. 1993, A&A, 274, 902
Tabatabaei, F. S., Beck, R., Krügel, E., et al. 2007, A&A, 475, 133
Teshima, M., et al. 2001, in Proc. 27th ICRC, ed. K.-H. Kampert, G. Hainzelmann, C. Spiering et al. (Lindau, Germany: Copernicus Gesellschaft), 337
van Eck, C. L., Brown, J. C., Stil, J. M., et al. 2011, ApJ, 728, 97
van Leeuwen, F., & Evans, D. W. 1998, Ap&SS, 130, 157
Völk, H. J., Zank, L. A., & Zank, G. P. 1988, A&A, 198, 274
Wiebel-Sooth, B., & Biermann, P. L. 1999, in Cosmic Rays, ed. K. Shaifers & H. H. Voigt (Berlin: Springer), 37
Wielen, R. 1975, in La Dynamique Des Galaxies Spirales, ed. L. Weliachew (Paris: CNRS), 357
Yoon, Y. S., Ahn, H. S., Allison, P. S., et al. 2011, ApJ, 728, 122
Yüksel, H., Kistler, M. D., & Stanev, T. 2009, PhRvL, 103, 051101
Yusef-Zadeh, F., & Morris, M. 1987, ApJ, 322, 721